Mode-coupling study on the dynamics of hydrophobic hydration

T. Yamaguchi,[a] T. Matsuoka, and S. Koda
Department of Molecular Design and Engineering, Graduate School of Engineering, Nagoya University, Chikusa, Nagoya, Aichi 464-8603, Japan

(Received 25 November 2003; accepted 26 January 2004)

The molecular motion of water in water–hydrophobic solute mixtures was investigated by the mode-coupling theory for molecular liquids based on the interaction-site description. When the model Lennard-Jones solute was mixed with water, both the translational and reorientational motions of solvent water become slower, in harmony with various experiments and molecular dynamics simulations. We compared the mechanism of the slowing down with that of the pressure dependence of the molecular motion of neat water [T. Yamaguchi, S.-H. Chong, and F. Hirata, J. Chem. Phys. **119**, 1021 (2003)]. We found that the decrease in the solvent mobility caused by the solute can essentially be elucidated by the same mechanism: That is, the fluctuation of the number density of solvent due to the cavity formation by the solute strengthens the friction on the collective polarization through the dielectric friction mechanism: We also employed the solute molecule that is the same as solvent water except for the amount of partial charges, in order to alter the strength of the solute–solvent interaction continuously. The mobility of the solvent water was reduced both by the hydrophobic and strongly hydrophilic solutes, but it was enhanced in the intermediate case. Such a behavior was discussed in connection with the concept of positive and negative hydrations.
 [DOI: 10.1063/1.1687319]

I. INTRODUCTION

The hydration of hydrophobic molecules, such as rare gases and hydrocarbons, is called ''hydrophobic hydration,'' and it has long been attracting many researchers. It is of academic interest due to its peculiar properties compared with other solvation processes, as will be described below. In addition, hydrophobic hydration is of great importance in biophysical fields, such as protein folding or membrane formation.

The hydrophobic hydration is characterized mainly by two properties: one is thermodynamic[1–18] and the other is dynamic.[19–39] Thermodynamically, the dissolution of a hydrophobic molecule into water is accompanied by both the entropic and enthalpic loss. Given that the direct interaction between the solute and solvent is weak, the negative solvation enthalpy is quite interesting, since a naive consideration predicts the enthalpic gain when the solute–solvent interaction is weak.

In order to elucidate the thermodynamics of the hydrophobic hydration, Frank and Evans proposed the ''iceberg'' model in 1945.[4] In this model, they proposed that the icelike structure is formed around the hydrophobic molecule, just as the crystalline hydrate. They connected the characteristic solvation thermodynamics to the ordering of the water molecules and the enhancement of the hydrogen-bonding structure between them. After the proposal of their model, many experimental,[40–43] theoretical[16–18,44,45] and computer simulation studies[2,12,13,33,34,46–55] have been performed to investigate the structural aspect of the hydrophobic hydration. Although it has been revealed that the word ''iceberg'' does not mean the rigid crystalline structure of ice I_h or hydrates exactly and that the relationship between the solvation structure and the partial thermodynamic quantities of a solute is not straightforward, the iceberg model is still regarded as the ''essentially'' correct picture of hydrophobic hydration.

The second characteristic of the hydrophobic hydration is the slowing down of the mobility of water molecules around the hydrophobic solutes. It also contradicts the naive consideration that the intermolecular interaction will be reduced on average by dissolving the solute molecule that interacts with the solvent weakly.

The experimental studies on the dynamics of the hydrophobic hydration have been performed mainly by nuclear magnetic resonance[19–27] or microwave[28–32] spectroscopies. The former measures the single-particle reorientational relaxation (by ^{2}H-NMR spin-lattice relaxation measurement) or the self-diffusion coefficient (by the field-gradient spin-echo measurement), while the latter does the dielectric relaxation that represents the collective reorientation of the electric dipole moment. Both experiments observe the decrease of the mobility of water molecules in solution on average, and the information on the hydration shell is extracted from the concentration dependence.

The dynamics of the hydrophobic hydration has also been studied by molecular dynamics (MD) simulations.[33–39] Contrary to the experiments, we can separately determine the dynamics of water molecules in the hydration shell in the MD simulation. In many simulations, it has been shown that the mobility of water in the shell is reduced by tens of a percent from that of bulk water.

Employing the idea of the iceberg model, the dynamics of the hydrophobic hydration has also been related to the

[a]Author to whom correspondence should be addressed. Electronic mail: tyama@nuce.nagoya-u.ac.jp

icelike structure of the hydration shell: That is, the molecular motion of water in the shell is reduced by the enhanced hydrogen-bonding structure of the shell. However, it is yet to be clarified what structure of the shell is responsible for the slowing down and how the structure affects the molecular mobility.

The molecular mobilities of aqueous ionic solutions,[56] such as the viscosity B coefficient[57,58] or the activation energy of the self-diffusion of water,[59] have also been discussed in relation to the solvation structure of ions. Small ions as Li^+ and Na^+ make the solvent mobility smaller. On the other hand, the relatively larger ions as Rb^+ and I^- tend to enhance the solvent mobility. Samoilov named the enhancement of the mobility of solvent water by ions ''negative hydration,'' whereas the solvation of smaller ions is called ''positive hydration.''[59] Much larger ions as tetraalkylammonium ones decrease the mobility of water, which is ascribed to the hydrophobic hydration.

The idea of positive and negative hydrations is often related to the ionic hydration model of Frank and Wen.[57] In their model, the small ions are surrounded by the region of structured water, called the A region, whereas the water just around the larger ions, called the B region, is more disordered than the bulk water. The order and disorder of the hydration shell has been related to the mobility of water in the shell. However, the questions also remain what the order and disorder mean and how they affect the mobility of water.

Recently, Yamaguchi *et al.* studied the pressure dependence of the molecular mobility of neat water by the mode-coupling theory.[60] They showed that the enhancement of the mobility by compression can be related to the suppression of the number-density fluctuation, rather than the breakdown of the tetrahedral hydrogen-bonding network structure. We extended their calculation to ionic liquids afterward and succeeded in explaining the anomalous pressure dependence of the transport properties of some ionic liquids in a similar way.[61,62]

In this work, we treat the mixture of water and hydrophobic model molecules in the same method, and the causality between the solvation structure and the mobility of water is discussed in terms of the mode-coupling theory. The MD simulations on some model solutions are also performed for the comparison with the theoretical calculation.

II. THEORY

A. Equilibrium structure

The mode-coupling calculation requires the equilibrium correlation functions of the liquid as one of the input parameters. In this work, we utilize the reference interaction-site model (RISM) integral equation[63–65] to obtain the static structure, as was the case of previous studies.[60–62]

The RISM integral equation theory consists of two equations. The first one is the site–site Ornstein–Zernike equation (RISM equation) described as

$$\tilde{\mathbf{h}}(k)=\tilde{\mathbf{w}}(k)\cdot\tilde{\mathbf{c}}(k)\cdot\tilde{\mathbf{w}}(k)+\tilde{\mathbf{w}}(k)\cdot\tilde{\mathbf{c}}(k)\cdot\boldsymbol{\rho}\cdot\tilde{\mathbf{h}}(k). \tag{1}$$

Here $\tilde{\mathbf{h}}(k)$, $\tilde{\mathbf{c}}(k)$, and $\tilde{\mathbf{w}}(k)$ stand for the total, direct, and intramolecular correlation functions, respectively, in the reciprocal space. The matrix of $\rho^{\alpha\gamma}$ is defined as $\rho_\alpha\delta_{\alpha\gamma}$, where $\alpha,\gamma,...$ refer to the interaction sites and ρ_α is the number density of the site α. The site–site static structure factor $\boldsymbol{\chi}(k)$ is defined and given by

$$\chi^{\alpha\gamma}(k)\equiv\frac{1}{V}\langle\rho^{\alpha *}(k)\rho^{\gamma}(k)\rangle=[\tilde{\mathbf{w}}(k)\cdot\boldsymbol{\rho}+\boldsymbol{\rho}\cdot\tilde{\mathbf{h}}(k)\cdot\boldsymbol{\rho}]_{\alpha\gamma}, \tag{2}$$

where $\rho^\alpha(k)$ is the density field of the α site in the reciprocal space. It should be noted here that our normalization factor of $1/V$ is different from literatures.

The second equation of the RISM integral equation theory is the closure one, which is the local relationship between the total and direct correlation functions. We use here the partially linearized hypernetted chain (PLHNC) closure proposed by Kovalenko and Hirata as[66]

$$\xi^{\alpha\gamma}(r)=-\beta u^{\alpha\gamma}(r)+h^{\alpha\gamma}(r)-c^{\alpha\gamma}(r), \tag{3}$$

$$g^{\alpha\gamma}(r)=\begin{cases}1+\xi^{\alpha\gamma}(r) & [\xi^{\alpha\gamma}(r)>0],\\ \exp[\xi^{\alpha\gamma}(r)] & [\xi^{\alpha\gamma}(r)<0],\end{cases} \tag{4}$$

where the functions without a tilde are those in the real space and $g^{\alpha\gamma}(r)\equiv h^{\alpha\gamma}(r)+1$ is the site–site radial distribution function. The interaction potential between sites α and γ is denoted as $u^{\alpha\gamma}(r)$ and β stands for $1/k_BT$, where k_B and T are the Boltzmann constant and absolute temperature, respectively. We employ the PLHNC closure in this work because its convergence is good especially in the case of mixture. We confirmed that the essential features of the results using the RISM/HNC equation are conserved by the replacement of the closure in the case of neat water.

B. Site–site mode-coupling theory

Under the assumption that only the site–density and site–current modes, denoted as $\rho^\alpha(k,t)$ and $\mathbf{j}^\alpha(k,t)$, respectively, are the slow variables of the system, we can derive the site–site generalized Langevin equation for mixtures of molecular liquids as

$$\ddot{\mathbf{F}}(k,t)+k^2\mathbf{J}(k)\cdot\boldsymbol{\chi}^{-1}(k)\cdot\mathbf{F}(k,t)+\int_0^t d\tau\,\mathbf{K}(k,t-\tau)\cdot\dot{\mathbf{F}}(k,\tau)=\mathbf{0}, \tag{5}$$

$$\ddot{\mathbf{F}}^s(k,t)+k^2\mathbf{J}^s(k)\cdot\mathbf{w}^{-1}(k)\cdot\mathbf{F}^s(k,t)+\int_0^t d\tau\,\mathbf{K}^s(k,t-\tau)\cdot\dot{\mathbf{F}}^s(k,\tau)=\mathbf{0}, \tag{6}$$

which are the natural extension of those of one-component molecular liquids[67] and simple-liquid mixtures.[68–70]

Here the site–site dynamic structure factor and its self-part in the time domain, denoted as $\mathbf{F}(k,t)$ and $\mathbf{F}^s(k,t)$, respectively, are defined as

$$F^{\alpha\gamma}(k,t)\equiv\frac{1}{V}\langle\rho^{\alpha *}(k,t=0)\rho^{\gamma}(k,t)\rangle, \tag{7}$$

$$F^{s,\alpha\gamma}(k,t)\equiv\frac{1}{N_\alpha}\langle\rho^{\alpha *}(k,t=0)\rho^{\gamma}(k,t)\rangle_s, \tag{8}$$

where N_α stands for the number of α sites and the suffix s means that the correlation between the quantities of different *molecules* is neglected. The site–current correlation matrix and its self-part $\mathbf{J}(k)$ and $\mathbf{J}^s(k)$, respectively, are defined in the same way as

$$J^{\alpha\gamma}(k) \equiv \frac{1}{V}\langle j_z^{\alpha *}(k,t=0) j_z^{\gamma}(k,t=0)\rangle, \tag{9}$$

$$J^{s,\alpha\gamma}(k) \equiv \frac{1}{N_\alpha}\langle j_z^{\alpha *}(k,t=0) j_z^{\gamma}(k,t=0)\rangle_s = \frac{1}{\rho_\alpha} J^{\alpha\gamma}(k), \tag{10}$$

where the z axis is taken parallel to the $\mathbf{k}$ vector.

The memory function matrices, denoted as $\mathbf{K}(k,t)$ and $\mathbf{K}^s(k,t)$, are the functions that describe the friction on the motion of interaction sites. In order to clarify the origin of the friction on the motion of molecules, we need to understand the memory functions on the molecular basis. The mode-coupling theory is the theory that approximates the memory function as the nonlinear function of the dynamic structure factor. As is done for one-component molecular liquids,[71,72] we can show the mode-coupling approximation of the memory function as follows:

$$\begin{aligned}[\boldsymbol{\rho}\cdot\mathbf{J}^{-1}(k)\cdot\mathbf{K}_{\mathrm{MCT}}(k,t)\cdot\boldsymbol{\rho}]_{\alpha\gamma} &= \frac{1}{8\pi^3}\int d\mathbf{q}\{q_z^2[\tilde{\mathbf{c}}(q)\cdot\mathbf{F}(q,t)\cdot\tilde{\mathbf{c}}(q)]_{\alpha\gamma}\mathbf{F}^{\alpha\gamma}(|\mathbf{k}-\mathbf{q}|,t) \\ &\quad - q_z(k-q_z)[\tilde{\mathbf{c}}(q)\cdot\mathbf{F}(q,t)]_{\alpha\gamma}[\mathbf{F}(|\mathbf{k}-\mathbf{q}|,t) \\ &\quad \cdot\tilde{\mathbf{c}}(|\mathbf{k}-\mathbf{q}|)]_{\alpha\gamma}\},\end{aligned} \tag{11}$$

$$\begin{aligned}[\mathbf{J}^{s,-1}(k)\cdot\mathbf{K}^s_{\mathrm{MCT}}(k,t)]_{\alpha\gamma} &= \frac{1}{8\pi^3}\int d\mathbf{q}\, q_z^2[\tilde{\mathbf{c}}(q)\cdot\mathbf{F}(q,t) \\ &\quad \cdot\tilde{\mathbf{c}}(q)]_{\alpha\gamma}\mathbf{F}^{s,\alpha\gamma}(|\mathbf{k}-\mathbf{q}|,t).\end{aligned} \tag{12}$$

Note that $\mathbf{J}^s(k)$ in Eq. (12) corresponds to $\mathbf{J}(k)$ in Refs. 60, 71, and 72 in the case of one-component liquids.

Yamaguchi and Hirata showed that, however, the mode-coupling expression of the memory function critically underestimates the friction on the reorientational motion of water.[73] They revealed that the underestimate of the friction is due to the neglect of the coupling between the different reorientational modes in a molecule, and they also proposed a modified expression of the memory function for one-component molecular liquids. In their modification, the memory function is described as the linear combination of that of the mode-coupling theory. We extend their modification to molecular liquid mixtures, which is described as

$$\begin{aligned}[\mathbf{K}^s(k,t)\cdot\mathbf{J}^s(k)]_{\alpha\gamma} &= \sum_{m_1,m_2,m_3\in\{x,y,z\}}\sum_{\mu\nu\in i}\langle u^{(i)}_{zm_1} Z^{\alpha\mu}_{m_1m_2} Z^{\nu\gamma}_{m_2m_3} u^{(i)}_{zm_3} \\ &\quad \times e^{i\mathbf{k}\cdot(\mathbf{r}_i^\alpha-\mathbf{r}_i^\mu-\mathbf{r}_i^\gamma+\mathbf{r}_i^\nu)}\rangle[\mathbf{J}^{s,-1}(k)\cdot\mathbf{K}^s_{\mathrm{MCT}}(k,t)]_{\alpha\gamma},\end{aligned} \tag{13}$$

which applies only when sites α and γ belong to the same molecule i and the mode-coupling memory function is used otherwise. In Eq. (13), $Z^{\alpha\gamma}_{m_1m_2}$ and $u^{(i)}_{zm}$ stand for the orientation-dependent site–site velocity correlation matrix and the unitary matrix that describes the rotation between the molecular- and laboratory-fixed coordinates of molecule i, respectively. The orientation dependence of the relationship between forces and acceleration is described by $Z^{\alpha\gamma}_{m_1m_2}$, and the coupling between different reorientational modes is taken into account by taking the autocorrelation between the accelerations *before* the orientational averaging is performed.

The collective part of the memory function is given by

$$\mathbf{K}(k,t) = \mathbf{K}_{\mathrm{MCT}}(k,t) + \mathbf{K}^s(k,t) - \mathbf{K}^s_{\mathrm{MCT}}(k,t), \tag{14}$$

as is the case of one-component molecular liquids.

C. Transport coefficients and relaxation times

In this work, we treat four dynamic quantities—shear viscosity, dielectric relaxation time, self-diffusion coefficient, and single-particle reorientational relaxation time—which can be measured by experiments. In this subsection, we present how these quantities are related to the dynamic structure factor obtained by the theory.

Yamaguchi and Hirata applied the mode-coupling approximation to neat molecular liquids and obtained the mode-coupling expression of the shear viscosity, η.[74] Their MCT expression can be easily extended to molecular liquid mixtures as

$$\eta = \int_0^\infty dt\, \eta(t), \tag{15}$$

$$\begin{aligned}\eta(t) \simeq \frac{k_BT}{60\pi^2}\int_0^\infty k^4 dk \mathrm{Tr}\Bigg[\Bigg\{\boldsymbol{\chi}^{-1}(k)\cdot\Bigg\{\frac{\partial\{\boldsymbol{\chi}(k)-\boldsymbol{\rho}\cdot\mathbf{w}(k)\}}{\partial k} \\ - \frac{\partial\mathbf{w}(k)}{\partial k}\cdot\{\boldsymbol{\chi}(k)-\boldsymbol{\rho}\cdot\mathbf{w}(k)\} - \{\boldsymbol{\chi}(k)-\boldsymbol{\rho}\cdot\mathbf{w}(k)\} \\ \cdot\frac{\partial\mathbf{w}(k)}{\partial k}\Bigg\}\cdot\boldsymbol{\chi}^{-1}(k)\cdot\mathbf{F}(k,t)\Bigg\}^2\Bigg].\end{aligned} \tag{16}$$

The complex electric permittivity $\epsilon(\omega)$ is related to the dynamic structure factor $\mathbf{F}(k,t)$ by Raineri *et al.* as[75]

$$\frac{1}{\epsilon_0} - \frac{1}{\epsilon(\omega)} = \lim_{k\to 0}\sum_{\alpha\gamma}\frac{4\pi i\omega z_\alpha z_\gamma}{k^2}\int_0^\infty dt\, e^{-i\omega t}F^{\alpha\gamma}(k,t), \tag{17}$$

where z_α is the partial charge on the site α and $\epsilon_0 \equiv \epsilon(\omega=0)$ is the static dielectric constant. In this work, the time-integrated dielectric relaxation time, denoted as τ_D, is defined as

$$\tau_D = \lim_{\omega\to 0}\frac{\epsilon''(\omega)}{\omega(\epsilon_0-\epsilon_\infty)}, \tag{18}$$

where $\epsilon''(\omega)$ and ϵ_∞ are the imaginary part of the complex permittivity (dielectric loss) and the dielectric constant at the infinite frequency, respectively. The value of τ_D in this definition is equal to the time-integrated relaxation time of the total dipole moment of the system under the conductive boundary condition[76] and also to the inverse of the peak frequency of the dielectric loss spectrum in the case of the

Debye relaxation. The value of ϵ_∞ is set unity in this work, which is consistent with our models of water and solute molecules that do not include the electronic polarizability.

The site–site velocity correlation function $\mathbf{Z}(t)$ is described in terms of the self-part of the dynamic structure factor $\mathbf{F}^s(k,t)$ as

$$Z^{\alpha\gamma}(t) \equiv \frac{1}{N_\alpha} \sum_i \langle \mathbf{v}^\alpha(0) \cdot \mathbf{v}^\gamma(t) \rangle_s = -\lim_{k\to 0} \frac{3}{k^2} \ddot{F}^{s,\alpha\gamma}(k,t). \tag{19}$$

Based on the Kubo–Green formula, the translational diffusion coefficient is easily obtained as[67,77]

$$D = \frac{1}{3} \int_0^\infty dt\, Z^{\alpha\gamma}(t). \tag{20}$$

In this expression, the sites α and γ can be chosen arbitrarily, as long as they are bound by chemical bonds.

The expression of the single-particle reorientational time is a little complicated.[60,77,78] For simplicity, we restrict our discussion to the rank-1 reorientational relaxation of the dipole moment $\boldsymbol{\mu}$ given by

$$\boldsymbol{\mu}_i = \sum_\alpha z_\alpha \mathbf{r}_i^\alpha. \tag{21}$$

The first-rank reorientational correlation function $C_{\boldsymbol{\mu}}(t)$ is defined as

$$C_{\boldsymbol{\mu}}(t) \equiv \frac{\Sigma_i \langle \boldsymbol{\mu}_i(t) \boldsymbol{\mu}_i(0) \rangle}{\Sigma_i \langle |\boldsymbol{\mu}_i^2| \rangle}. \tag{22}$$

Substituting Eq. (21) into Eq. (22), $C_{\boldsymbol{\mu}}(t)$ is related to the site–site velocity correlation function $\mathbf{Z}(t)$ as

$$C_{\boldsymbol{\mu}}(t) = \frac{\Sigma_i \Sigma_{\alpha\gamma} z_\alpha z_\gamma \langle \mathbf{r}_i^\alpha(t) \cdot \mathbf{r}_i^\gamma(0) \rangle}{\Sigma_i \langle |\boldsymbol{\mu}_i^2| \rangle}, \tag{23}$$

$$\ddot{C}_{\boldsymbol{\mu}}(t) = -\frac{N \Sigma_{\alpha\gamma} z_\alpha z_\gamma Z^{\alpha\gamma}(t)}{\Sigma_i \langle |\boldsymbol{\mu}_i^2| \rangle}, \tag{24}$$

where N means the number of molecules. The reorientational correlation time of the first rank, τ_μ, shall be defined as the time integration of $C_{\boldsymbol{\mu}}(t)$.

III. MODELS

We employed the extended simple point charge (SPC/E) model[79] as the structure and the intermolecular potential of water. We put the Lennard-Jones (LJ) cores on the hydrogen atoms in order to avoid the undesired divergence of the solution of the RISM integral equation. The LJ parameters of the hydrogen atom—the depth of the well and the diameter—are chosen to be 0.046 kcal/mol and 0.7 Å, respectively, as is the case of the study of neat water by Yamaguchi *et al.*[60]

Two types of solute molecules are treated. The first one is the neutral LJ particle whose LJ parameter is the same as that of O atom of the SPC/E potential. The mass of the solute is set to be 18 in atomic units, which is equal to the total mass of the solvent water. For the first type of solute, we changed the molar fraction of the solute from 0 to 0.1. The LJ particle is used as a model of rare gases or methane. This solution is hereafter called the ''hydrophobic solution.'' For comparison with the hydrophobic solution, we also perform calculation on the neat water of reduced density, hereafter called ''stretched water,'' whose number density of water is the same as that of the hydrophobic solution.

The second one is the model triatomic molecule, whose geometry, inertia parameters, and LJ parameters of sites are the same as those of SPC/E water. The solute differs from the solvent only in their partial charges on sites. In the SPC/E model, the partial charges on H atoms are $\delta e_0 \equiv 0.4238e$ ($-e$ stands for the charge of the electron) and $-2\delta e_0$ is placed on the O atom. In our model solutes, the charges of δe and $-2\delta e$ are put on the H and O atoms, respectively, and the value of δe is varied from 0 to $0.5e$. We can vary the hydrophobicity of the solute by changing the value of δe. In particular, the LJ solute in the first model ($\delta e = 0$) and neat water ($\delta e = \delta e_0$) are continuously connected in this model. We call this model solute ''waterlike solute.'' For the second type of solute, the molar fraction of the solute is fixed to be 0.1.

In all the calculations, the temperature of the system is 298 K, and the number density is 0.033 34 molecules/Å^3, which is equal to that of neat water at the ambient condition. It is to be noted that, since the partial molar volume of the solute depends not only on the size of the repulsive core, but also on the intermolecular attractive interaction, the addition of solute molecules with fixed total number density in this study may not correspond exactly to the isobaric condition in usual experiments.

IV. NUMERICAL METHODS

A. Mode-coupling calculation

Combining the generalized Langevin-modified mode-coupling theory and the RISM/PLHNC integral equation theory, we can evaluate the transport coefficients and the relaxation times of liquids and liquid mixtures based solely on the information of molecular shapes, inertia parameters, intermolecular interaction potentials, temperature, density, and concentration.

First, the site–site static structure factor is obtained by the RISM/PLHNC equation from the intermolecular interaction, molecular shape, temperature, density, and concentration. No dielectric correction, such as the Stell correction[80] or the dielectrically consistent RISM (DRISM) theory,[81] is employed, since we have no information on the dielectric constant of the model system. Although the small dielectric constant of RISM/PLHNC theory affects the absolute value of the dielectric relaxation time through the Kirkwood g factor, we consider that its effect on the relative change of τ_D and other properties is small. We use the modified direct inversion in an iterative space DIIS method proposed by Kovalenko *et al.* in order to improve the convergence of the RISM calculation.[82]

From the static site–site structure factor, we calculate the site–site dynamic structure factor using the site–site generalized Langevin-modified mode-coupling theory. The gener-

alized Langevin equation is time integrated numerically. The time development of the correlation function in the hydrodynamic limit $k \to 0$ is separately treated by the analytical limiting procedure of the theoretical expressions.

In the numerical procedure, the reciprocal space is linearly discretized as $k=(n+\frac{1}{2})\Delta k$, where n is an integer from 0 to N_k-1. The values of Δk and N_k are 0.245 Å^{-1} and 128, respectively. Although the value of N_k appears rather small, the improvement of the correlation functions in the reciprocal space is rather small with larger values, and we employed $N_k=128$, because the calculation involving 6×6 matrix in the mode-coupling calculation is numerically demanding.

B. Molecular dynamics simulation

The molecular dynamics simulations on the second type of model solutes (waterlike solutes) are performed in order to test the validity of our theoretical calculation. The system consists of 256 molecules: 26 of them are the solute molecules and the remaining 230 are the solvent water. The molar fraction of the solute is thus approximately 0.1. The simulation cell is cubic, and the periodic boundary condition is employed. The simulation is performed under the *NVE*-constant ensemble. The long-range Coulombic interaction is evaluated by the Ewald method.[83] The short-range force is cut off at the half length of the cell. The reorientational degree of freedom is described by the quaternion,[83] and the equation of motion is integrated by the algorithm proposed by Matubayasi and Nakahara.[84] The length of the time step is 1 fs. After the equilibration run of 100 ps length, the simulation run is continued for 1 ns to calculate the correlation functions. The linear and angular velocities are scaled many times during the equilibration run to adjust the temperature of the system to the target value, 298 K, and no temperature control is performed after the equilibration. The average temperature is controlled within ±5 K, and we found no systematic correlation between the fluctuation of temperature among different runs and the mobility of water. The translational diffusion coefficient of the solvent water is obtained from the slope of the mean-square displacement of the oxygen atom.

V. RESULTS AND DISCUSSIONS

A. Lennard-Jones solutes

Figure 1 shows the relative decrease in the molecular mobility of water with increasing the concentration of the Lennard-Jones solute, which appears as the change in the shear viscosity, dielectric relaxation time, the self-diffusion coefficient, and the single-dipole reorientation time of solvent water. All these values indicate that the mobility of solvent water is reduced by the addition of solute, in harmony with experimental and simulation observations that the motion of water slows down around hydrophobic solutes.

Comparing the translational and reorientational mobilities of water, it is found that the effect of the hydrophobic solute is larger on the reorientation than on the translation, as is the case of the pressure effect on neat water.[60] The enhancement of the viscosity is smaller than the decrease in the translational diffusion coefficient of water, which we consider is because the motion of solute is involved in the transverse collective momentum density.

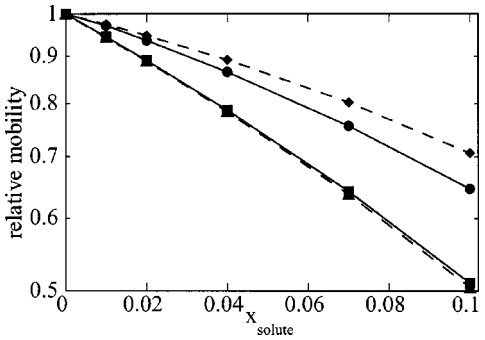

FIG. 1. Relative mobility of the solvent water as the functions of the molar fraction of the Lennard-Jones model solutes, x_{solute}. Circle: D/D_0. Square: $\tau_{\mu,0}/\tau_\mu$. Triangle: $\tau_{D,0}/\tau_D$. Diamond: η_0/η, where D, τ_μ, τ_D, and η stand for the translational diffusion coefficient, single-dipole reorientation time, dielectric relaxation time, and shear viscosity, respectively, and the symbols with suffices "0" represent the respective values of neat ambient water. Note that the longitudinal axis is plotted in a logarithmic scale. The squares and triangles are almost overlapped with each other.

The relative mobility of water decreases linearly with the solute concentration in the dilution limit, and it depends on the concentration rather smoothly. It indicates that the reduction of the mobility stems from the solvation structure around a solute, rather than the association of the solutes. The solute–solute radial distribution function also shows that the significant association of the solute molecules is not present in the static structure. We will analyze hereafter mainly the result of the molar fraction of 0.1 for numerical reasons, considering that the decrease in the mobility observed there reflects the effect of the solvation structure of a solute.

As is commented in Sec. I, Yamaguchi *et al.* succeeded in reproducing qualitatively the anomalous pressure dependence of the molecular mobility of neat water by the mode-coupling theory.[60] They also proposed that the decrease in the friction with increasing density originates in the suppression of the number-density fluctuation in the low-q region. Hereafter we will compare the dynamics of water in solution of the hydrophobic solute with that of stretched water. Although the hydrophobic solution and stretched water are quite different from each other on experimental views, they have the common property that the intermolecular distance is enlarged on average compared with that of neat ambient water. The difference is only that there are solute molecules between solvent water molecules in the case of solution, whereas only the vacancy (vacuum) exists in the stretched water.

Based on this view point, we compare the numerical results on three systems. The first one is the neat water at the ambient density. The second one is the hydrophobic solution whose solute molar fraction is 0.1. The last one is the neat stretched water whose density is reduced to 90% of the ambient one. The last system is chosen so that the number density of water is equal to that of the second one.

Figure 2(a) shows the radial distribution function between oxygen and hydrogen atoms of solvent water, denoted

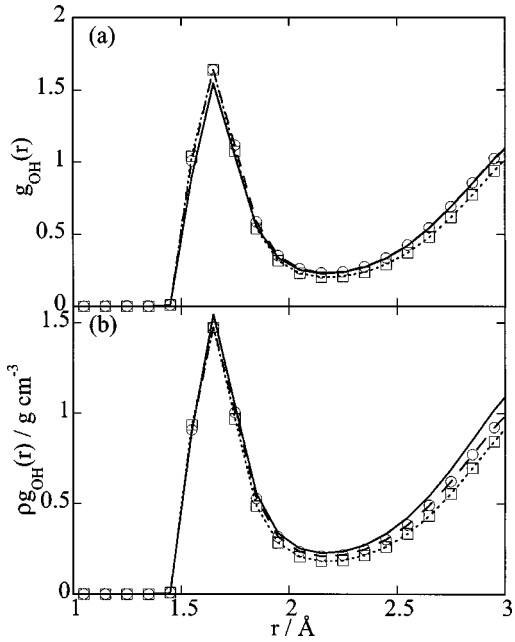

FIG. 2. Static distribution functions between solvent water molecules in three model systems—that is, neat ambient water (solid curve), hydrophobic solution (dashed curve with circles), and neat stretched water (dotted curve with squares). In (a), the radial distribution functions, $g_{OH}(r)$ between solvent molecules are plotted, and they are multiplied by the number density of the solvent in (b).

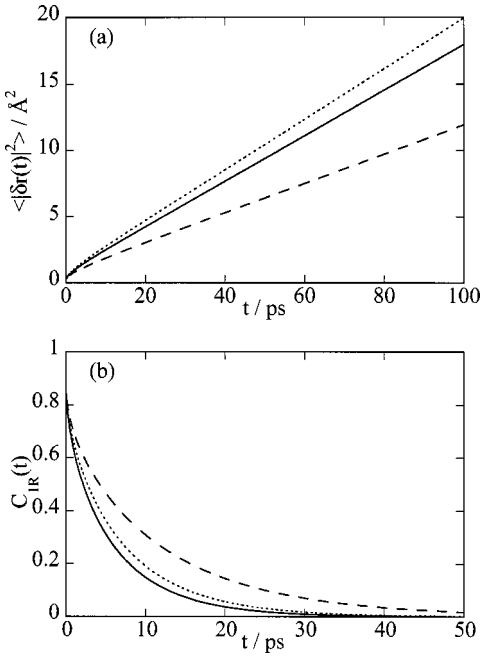

FIG. 3. Time correlation functions of three model systems. The solid, dashed, and dotted curves refer to the neat ambient water, hydrophobic solution, and neat stretched water, respectively. The mean-square displacements and the rank-1 reorientational correlation functions are shown in (a) and (b), respectively.

as $g_{OH}(r)$, of these liquids. The peak around 1.7 Å stands for the hydrogen bonding between water molecules. The hydrogen-bonding peaks of the solution and stretched water are similar, and both are higher than that of neat ambient water. The increase in the peak height appears consistent with a prevailed idea that the hydrogen-bonding network structure is enhanced by both the stretching and the addition of the hydrophobic solutes. The hydrogen-bonding probability between a pair of neighbor water molecules within the hydration shell is actually confirmed by the simulation.[51] However, the local number density of oxygen atoms around a hydrogen atom is described as $\rho g_{OH}(r)$, where ρ stands for the bulk density of water, and the increase in the peak of the radial distribution function may not mean that in the *number* of the hydrogen bonding per a water molecule, because ρ decreases with an increase in the concentration of solutes.

Figure 2(b) exhibits $g_{OH}(r)$ multiplied by ρ. It stands for the local site density of different molecules, and the integration of the peak is directly related to the coordination number. As is shown in the figure, the *decrease* of the peak height is observed in the hydrophobic solution after multiplication of the bulk solvent density. It indicates that the *number* of hydrogen bonding per water molecule *decreases* in the solution if we employ the O–H distance as the criteria of the hydrogen bonding.

Here we shall comment on the fact that the decrease in the number of hydrogen bonding is not an artifact of the integral equation theory. There have been many molecular simulation to examine the hydrogen bonding of water within the hydrophobic hydration shell. Some studies report the increase in hydrogen-bonding number, and others do otherwise.[13,33,34,46–55] As shall be shown later, the decrease in the coordination number is also observed in our MD simulation of the corresponding system. In NMR experiments, the enhancement of the spin-lattice relaxation rate of nuclei of solvent water by hydrophobic solutes is found in various systems, while the chemical shift of the protons of water does not always exhibit the lower-field shift (lower-field shift of proton usually corresponds to the larger polarization of the O–H bond).[19,20] Recently, Soper and co-workers measured the atomic radial distribution functions of mixtures by the neutron and x-ray scattering experiments, and they reported that the significant increase in the *number* of hydrogen bonding is not observed by the introduction of hydrophobic molecules.[40–43]

Anyway, the mobility of the solvent water is reduced by the model hydrophobic solute in our present calculation, as opposed to the decrease in the coordination number. It indicates that the decrease in the mobility of water is a highly collective phenomenon, and our theory captures the collective nature well.

The mean-square displacements and the single-particle reorientational correlation functions of water in the three systems are plotted in Figs. 3(a) and 3(b), respectively. As is shown in Fig. 1, both the translational and reorientational mobilities decrease in solution compared with water at the ambient density.

The translational diffusion coefficient of the stretched water is slightly larger than that of the ambient water in the present calculation. Although the translational mobility of real water is an increasing function of pressure at the ambient temperature, the anomaly in the translational mobility is underestimated in our theory, as was shown in the previous study of Yamaguchi *et al.*[60] The reorientational relaxation of

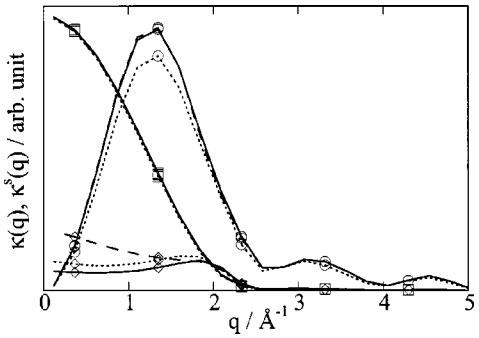

FIG. 4. Wave-number resolved memory function at the time zero. Circles and squares refer to the translational and single-dipole reorientational components of $\kappa^s(q)$, respectively, and diamonds refer to the dielectric component of $\kappa(q)$. The definitions of $\kappa(q)$ and $\kappa^s(q)$ are given by Eqs. (27) and (28), respectively. The functions of neat ambient water, hydrophobic solution, and neat stretched water are shown as the solid, dashed, and dotted curves, respectively.

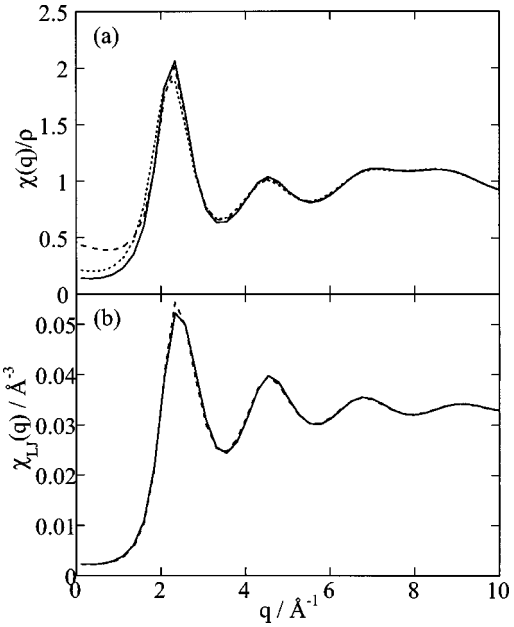

FIG. 5. Number-density fluctuation of three model systems—the neat ambient water (solid curve), hydrophobic solution (dashed curve), and neat stretched water (dotted curve). In (a), the z^2-weighted static structure factor divided by the density of water is plotted. In (b), the static structure factors of the LJ core, defined as Eq. (31) of neat ambient water and hydrophobic solution, are compared.

the stretch water is slower than that of the ambient one, as is the case of the previous study. Comparing the stretched water with the water in the hydrophobic solution, the latter is less mobile than the former, which is naturally understood as excess friction due to the repulsive interaction between water and the LJ particle (solute).

According to the previous mode-coupling study of compressed water, we shall analyze how the hydrophobic solute reduces the mobility of solvent water from the analysis of the integrand of the mode-coupling memory function. The mode-coupling memory function on the hydrodynamic modes, $k=0$, is expressed as

$$\lfloor \boldsymbol{\rho}\cdot\mathbf{J}^{-1}(k=0)\cdot\mathbf{K}_{\mathrm{MCT}}(k=0,t)\rfloor = \int_0^\infty 4\pi q^2 \boldsymbol{\kappa}(q,t)\,dq, \tag{25}$$

$$\lfloor \mathbf{J}^{s,-1}(k=0)\cdot\mathbf{K}_{\mathrm{MCT}}(k=0,t)\rfloor = \int_0^\infty 4\pi q^2 \boldsymbol{\kappa}^s(q,t)\,dq, \tag{26}$$

where $\boldsymbol{\kappa}(q,t)$ and $\boldsymbol{\kappa}^s(q,t)$ denote the contribution of the structure of each wave number to the time-dependent friction, which are given by

$$\kappa^{\alpha\gamma}(q,t) = \frac{1}{24\pi^2\rho_\alpha} q^2 \{\lfloor \tilde{\mathbf{c}}(q)\cdot\mathbf{F}(q,t)\cdot\tilde{\mathbf{c}}(q)\rfloor_{\alpha\gamma} F^{\alpha\gamma}(q,t) - \lfloor \tilde{\mathbf{c}}(q)\cdot\mathbf{F}(q,t)\rfloor_{\alpha\gamma}\lfloor \mathbf{F}(q,t)\cdot\tilde{\mathbf{c}}(q)\rfloor_{\alpha\gamma}\}, \tag{27}$$

$$\kappa^{s,\alpha\gamma}(q,t) = \frac{1}{24\pi^2} q^2 \lfloor \tilde{\mathbf{c}}(q)\cdot\mathbf{F}(q,t)\cdot\tilde{\mathbf{c}}(q)\rfloor_{\alpha\gamma} F^{s,\alpha\gamma}(q,t). \tag{28}$$

In the present mode-coupling calculation, the static structure is reflected in the short-time part of the memory function at first, which affects the relaxation of a mode, and the change in the dynamics of the mode influences the relaxation of other modes as a secondary effect. Therefore, we can realize the primary relationship between the static structure and the dynamics of various modes from the analysis of the short-time part of the memory function. In particular, $\boldsymbol{\kappa}(q) \equiv \boldsymbol{\kappa}(q,t=0)$ and $\boldsymbol{\kappa}^s(q) \equiv \boldsymbol{\kappa}^s(q,t=0)$ are given by the static structure factor, and we shall discuss the origin of the dynamics of the hydrophobic hydration based on these functions.[60]

Figure 4 shows the dielectric part of $\boldsymbol{\kappa}(q)$ and the solvent translational and reorientational parts of $\boldsymbol{\kappa}^s(q)$ for the three systems: the ambient water, hydrophobic solution, and stretched water.

The short-time friction on the single-particle translation decreases upon stretching, which is consistent with the previous study.[60] On the other hand, the short-time friction on the translational diffusion is similar for the ambient water and solution. It indicates that the value of the translational part of $\boldsymbol{\kappa}^s(q)$ is dominated by the repulsive interaction between the LJ cores, which is consistent with the difference in the translational diffusion of water in the stretched system and hydrophobic solution. However, the slowing down of the translational diffusion of water in solution compared with the neat ambient water is not explained by the translational part of $\boldsymbol{\kappa}^s(q)$, and we consider it is the secondary effect caused by the coupling with other modes.

The solvent reorientational part of $\boldsymbol{\kappa}^s(q)$ is almost the same for the three systems. Therefore, we need to consider the effect of the dynamics of other modes to explain the differences in the single-particle reorientational relaxation of water as is shown in Fig. 3(b).

The dielectric part of $\boldsymbol{\kappa}(q)$ varies strongly among the three systems. In particular, the function at $q<2\ \mathrm{Å}^{-1}$ changes largely, in accordance with the variation of the mobilities. In the study of the dynamics of compressed water, Yamaguchi *et al.* ascribed the anomalous pressure dependence of the mobility to this change in the friction on the dielectric mode.[60] The increase in the low-q structure of the

dielectric component of $\kappa(q)$ lengthens the dielectric relaxation time, and the slow dielectric relaxation in turn enhances the friction on other modes through the dielectric friction. The increase in the low-q part is larger for the hydrophobic solution than for the stretched water, which also corresponds to the lower mobility of the former than the latter.

The low-q contribution of the memory function mainly comes from the intermolecular Coulombic interaction. In order to understand the change in the dielectric part of $\kappa(q)$ qualitatively, we replace the direct correlation function in Eq. (27) with the Coulombic interaction as

$$\tilde{c}^{\alpha\gamma}(q) \to \frac{4\pi\beta z_\alpha z_\gamma}{q^2} \quad (q \to 0). \tag{29}$$

After the substitution, the dielectric part of $\kappa(q)$ is given by

$$\begin{aligned}\sum_{\alpha\gamma} z_\alpha z_\gamma \kappa^{\alpha\gamma}(q) &\to \frac{1}{6\pi^2 k_B T \rho}\left[\sum_{\alpha\gamma} z_\alpha^2 z_\gamma^2 \chi^{\alpha\gamma}(q)\right] \\ &\times\left[\frac{4\pi}{k_B T}\sum_{\alpha\gamma} z_\alpha z_\gamma \chi^{\alpha\gamma}(q)\right] \\ &= \frac{1}{6\pi^2 k_B T \rho}\left[\sum_{\alpha\gamma} z_\alpha^2 z_\gamma^2 \chi^{\alpha\gamma}(q)\right] \\ &\times\left[1-\frac{1}{\epsilon_L(q)}\right],\end{aligned} \tag{30}$$

where ρ means the number density of water. Here we used the property of the three systems that only the solvent water has partial charges. In the second line, $\epsilon_L(q)$ stands for the wave-number-dependent longitudinal dielectric function.

The second factor of the right-hand side of Eq. (30) in the low-q region is mainly determined by the intermolecular Coulombic interaction in the case of highly polar liquids, and it is almost independent of the liquid density or the solute concentration. The small dependence is actually confirmed in our numerical calculation.

On the other hand, the first term is strongly dependent among three systems, as is shown in Fig. 5(a). The z^2-weighted number-density fluctuation of the stretched water is larger than that of the ambient water at $q<2$ Å^{-1}, which means that the liquid becomes more compressible due to the looser packing of the stretched water. The solvent number-density fluctuation of the hydrophobic solution is further enhanced in the low-q region. According to Eq. (30), this increase in the fluctuation is the reason for the increase in the dielectric component of $\kappa(q)$ in the low-q region, which makes the dielectric relaxation of the solution slower.

In order to understand the origin of the enhanced fluctuation of the solvent number density, we construct the static structure factor of the LJ cores, irrespective of those of solutes and solvents, as is shown in Fig. 5(b). The definition of the structure factor of the LJ core, denoted as $\chi_{\mathrm{LJ}}(q)$, is given by

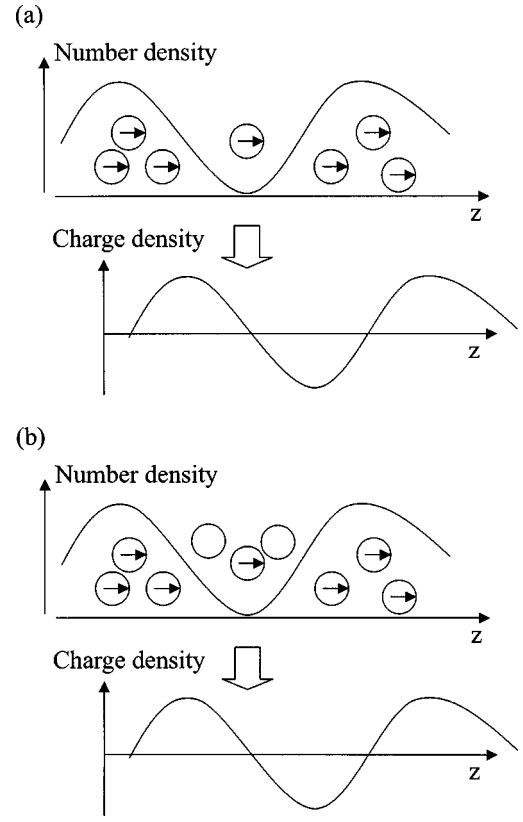

FIG. 6. Schematic picture on the electrostatic friction on the dielectric modes of (a) stretched water and (b) hydrophobic solution. In the stretched water, thermal fluctuation of the number density is enhanced due to the loose packing, as shown in the upper panel of (a). When the polar molecules reorients uniformly to the z direction, the heterogeneity of the polarization density is induced by the number-density fluctuation. Since the heterogeneous polarization, which is equivalent to the charge density, requires excess electrostatic energy, the number-density fluctuation leads to electrostatic friction on the dielectric mode. Although the packing of the hydrophobic solution is not so loose, the number density of the polar solvent fluctuates due to the cavity formation of the nonpolar solutes, as shown in the upper panel of (b), and this fluctuation works in the same way as the number-density fluctuation of the stretched water in (a).

$$\begin{aligned}\chi_{\mathrm{LJ}}(q) &\equiv \frac{1}{V}\langle\{\rho_{\mathrm{O}}^*(q)+\rho_{\mathrm{LJ}}^*(q)\}\{\rho_{\mathrm{O}}(q)+\rho_{\mathrm{LJ}}(q)\}\rangle \\ &= \sum_{i,j\in\{\mathrm{O,LJ}\}} \chi^{ij}(q),\end{aligned} \tag{31}$$

where $\rho_{\mathrm{O}}(q)$ and $\rho_{\mathrm{LJ}}(q)$ stand for the density fields of the O atom of the solvent water and the LJ solute, respectively. As is clearly demonstrated there, the number-density fluctuation of the LJ core of the solution is as small as that of the ambient water in the low-q region. Therefore, the fluctuation of the solvent density is enhanced because the solvent is partly replaced by the solute. Due to the excluded volume of the solute molecule, the solute makes places where solvent molecules cannot enter, which appears as the fluctuation of the solvent density.

Figure 6 exhibits a schematic picture on the physical mechanism of the electrostatic friction on the dielectric relaxation. Pictures on the stretched water and the hydrophobic solution are shown in (a) and (b), respectively, for comparison. Consider that the uniform electric field is applied to the

neat polar liquid along the z axis, as in Fig. 6(a). The polar molecules tend to align the direction of the external field. When the number density of the liquid is not uniform, the uniform polarization of molecules causes the nonuniform polarization density, which means the heterogeneity of the charge density. The presence of the charge density then causes the excess electrostatic energy, leading to the electrostatic friction on the dielectric relaxation.

Now we turn to the hydrophobic solution, as is shown in Fig. 6(b). Since the hydrophobic solution is more tightly packed than the stretched water, the fluctuation of the number density of the molecules *as a whole*, irrespective of solutes and solvents, is smaller. However, if we focus the polar molecules only, its number density fluctuates more largely in the solution. Since only the polar molecules can contribute to the orientational polarization, the heterogeneous distribution of the polar molecules can induce electrostatic friction on the dielectric mode, as is the case of the stretched water explained above.

In short, cavity formation by the solute increases the solvent number-density fluctuation, which enhances the electrostatic friction on the dielectric relaxation. Due to the slowing down of the dielectric relaxation, the mobility of water molecules in solution is reduced through the dielectric friction mechanism.

Although our present picture appears different from the conventional one—that the structural formation around the hydrophobic solute is the reason for the slow dynamics in the hydration shell—we cannot talk of consistency unless the meaning of ''structural formation'' in the conventional picture is specified. We consider our present study will help clarifying what structure around the shell is responsible for the dynamics of hydrating water. Also, we would like to note here that our result on the *dynamics* of the hydrophobic hydration appears consistent with a theory on the *thermodynamics* of the hydrophobic hydration that stresses on the role of the cavity formation by the solute.[5,6]

We shall here comment on the role of the peak structure around $q\sim 2\ \text{Å}^{-1}$ in the dielectric component of $\kappa(q)$. In our previous study on the silica melt, the similar structure is also found around $q\sim 2\ \text{Å}^{-1}$, which corresponds to the position of the prepeak of the static structure factor.[62] The prepeak is the fluctuation of the number density without accompanying that of the charge density, and it is considered to be associated with the SiO_2 tetrahedral unit of the silica melt. In the previous study, we have shown that the decrease in the prepeak with increasing density is responsible to the enhancement of the mobility and that the decrease in the prepeak can be interpreted as the increase in the five-coordinated silicon atom. Although the prepeak structure is not apparent in the site–site structure factor of water from the RISM/HNC or RISM/PLHNC integral equation theories, it is present around $q\sim 2\ \text{Å}^{-1}$ in the structure factor from the x-ray scattering or molecular simulations. Therefore, there is a possibility that the effect of the tetrahedral network structure of water is found in the dielectric component of $\kappa(q)$ around $q\sim 2\ \text{Å}^{-1}$. However, as is demonstrated in Fig. 4, the enhancement of the friction on the dielectric mode of hydrophobic solution comes from the lower-q region, $q<1.5\ \text{Å}^{-1}$, and the contribution of the peak around $q\sim 2\ \text{Å}^{-1}$ is slightly smaller than that of ambient water. The slowing down of the mobility of water in solution can therefore not be attributed to the strengthening of the tetrahedral structure of water even in this sense, although this conclusion may be dependent on the deficiency of the integral equation theory to describe the static structure.

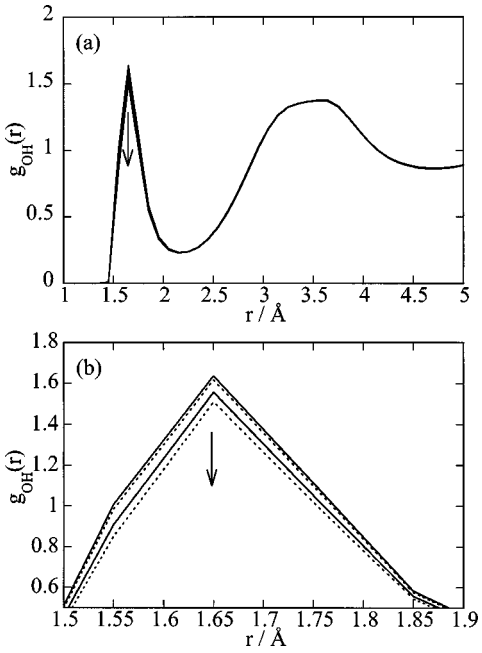

FIG. 7. Solvent–solvent $g_{OH}(r)$ of the aqueous solution of waterlike solutes. The arrow indicates the direction of increasing δe. The values of δe are, from upper to lower, 0, $0.2e$, $0.4e$, and $0.5e$, respectively. The peaks are enlarged in (b) to show the changes clearly.

B. Waterlike solutes: Theory

We shall present in this subsection the results of the theoretical calculation on the aqueous solution of model waterlike solutes.

Figure 7 exhibits the radial distribution functions between O and H atoms of *solvent* molecules. The hydrogen-bonding peak is enlarged in Fig. 7(b), since the change in the peak height is small. As shown in the figures, the peak of $g_{OH}(r)$ becomes larger as the partial charges on the sites of solute decrease. The increase in the peak height of $g_{OH}(r)$ can be thought as the sign of the structural enhancement, so as to compromise our numerical results with the conventional picture that the hydrogen bonding between solvent molecules in the hydration shell is stronger around the more hydrophobic solutes.

The diffusion coefficient and the reorientational relaxation time of the solvent water, and the viscosity of the solution, obtained by the mode-coupling calculation, are plotted in Fig. 8. The mobilities are normalized by the values of the neat water. As shown in the figure, the mobility of solvent water has a maximum value around $\delta e=0.3e$. When the solute–solvent interaction is stronger than the solvent–solvent one, the solvent molecules move less easily in the hydration shell than in the bulk. As the solute–solvent inter-

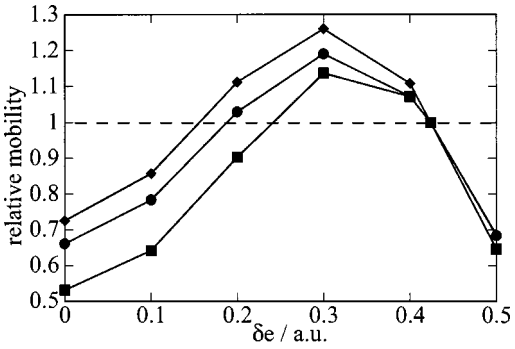

FIG. 8. Relative mobilities of the aqueous solution of the model waterlike solutes as the functions of the partial charges of the solute, δe. Circles and squares stand for D/D_0 and $\tau_{\mu,0}/\tau_\mu$, and diamonds do η_0/η, where "0" indicates the value of the neat ambient water.

action becomes weaker, the suppression of the mobility becomes weaker, and the motion of the water in the shell speeds up when the solute–solvent interaction becomes weaker than the solvent–solvent one. However, as the solute becomes hydrophobic further, the mobility of the solvent water decreases again, and it finally falls below that of neat water.

The existence of the maximum in the dependence of the water mobility on the water–solute interaction strength has been reported in many systems. For example, as has been introduced in Sec. I, the mobility of water in the hydration shell of univalent cations, as appears in the viscosity or NMR B coefficients and the self-diffusion coefficient of water, is larger than that of bulk one in the case of ions with intermediate size (e.g., K^+), whereas both smaller (e.g., Li^+) and larger (e.g., tetraalkylammonium) ions make the mobility of water lower.[56–59] As for aqueous solutions of organic molecules, the slowing down of hydrating water is larger for more hydrophobic solutes. For example, Nakahara and Yoshimoto reported that the NMR B coefficient of benzene is positive, while that of phenol is negative.[26] Kaatze and Pottel showed that the dielectric B coefficient is larger for more hydrophobic solutes within a series of methyl-substituted azo compounds or urea derivatives.[28]

In analogy with the ionic size dependence of the NMR (Ref. 56) or viscosity B coefficients,[58] we can define three regions of the solute–solvent interaction as follows. The first one is the "positive hydration," where the solvent motion is hindered by the strong solute–solvent interaction ($\delta e \geqslant \delta e_0$). The second one is the "negative hydration" ($0.2e \leqslant \delta e \leqslant \delta e_0$), and the last one is the "hydrophobic hydration" ($\delta e \leqslant 0.2e$). The border between the negative and hydrophobic hydration regions is dependent on the values of interest, as is shown in Fig. 8. Although some people may question our usage of the terms of "positive" and "negative" hydrations, we consider that it does not deviate from the original definition by Samoilov so much, since he defined the positive and negative hydrations according to the effect of ions on the mobility of water in his original paper.[59]

The positive-hydration region can be understood as the result of strong solute–solvent interaction. We have just analyzed the dynamics of the hydrophobic hydration in the previous subsection and concluded that it is due to the enhancement of the electrostatic friction on the dielectric mode caused by the cavity formation by the solute. However, the existence of the region of negative hydration is somewhat puzzling. The dynamics of the negative hydration is usually attributed to the structure-breaking effect of the solute. According to Fig. 7, however, the hydrogen-bonding peak of $g_{OH}(r)$ between solvent molecules increases monotonically with decreasing δe. If we consider that the enhancement of the hydrogen-bonding peak of the radial distribution function in the hydrophobic region as the sign of the structure formation and that such a structure formation is the reason for the slowing down of the solvent mobility, therefore, we have to expect the *decrease* in the mobility of water also in the negative-hydration region, contrary to the theoretical result in Fig. 8.

Based on our novel interpretation of the dynamics of hydrophobic hydration, we shall present a picture that describes the δe dependence of the solvent mobility in the whole region qualitatively. Remember first that the dynamics of the hydrophobic hydration is caused by the fluctuation of the number density of the molecules with strong Coulombic interaction, as shown in the previous subsection. Since it is the effect of the fluctuation, it behaves as $O((\delta e - \delta e_0)^2)$ when δe is close to δe_0. On the other hand, there is an effect of δe that behaves as $O(\delta e - \delta e_0)$, which describes the weakening of the intermolecular interaction of the solution on average. Matsubayashi and Nakahara discussed such an effect on dynamic properties based on the first-order perturbation theory.[85] Since the solute–solvent interaction is an increasing function of δe, the first-order effect works so as to enhance the mobility of solvent water when the value of δe is small.

The presence of the "negative" and "hydrophobic" hydration regimes can be realized in terms of the competition between the first- and higher-order effects. When the value of δe is slightly smaller than that of δe_0, the first-order effect dominates the higher-order one, and the mobility of solvent water is enhanced, which corresponds to the "negative-hydration" region. On the other hand, the higher-order effect of hydrophobic hydration can be larger than the first-order one and the solvent motion is hindered in the case of the strongly hydrophobic solutes.

In summary, the results on the series of the model solutes can be understood in the following manner. In the "positive-hydration" region, the mobility of the solvent water is suppressed by the strong solute–solvent interaction. In the "negative-hydration" region, where the solute–solvent interaction is slightly smaller than the solvent–solvent one, the motion of water is enhanced due to the weakening of the intermolecular interaction on average. When the solute becomes very hydrophobic, the effect of the electrostatic friction caused by the cavity formation overcomes the weakening of the intermolecular interaction on average, and the solvent water becomes less mobile compared with neat water.

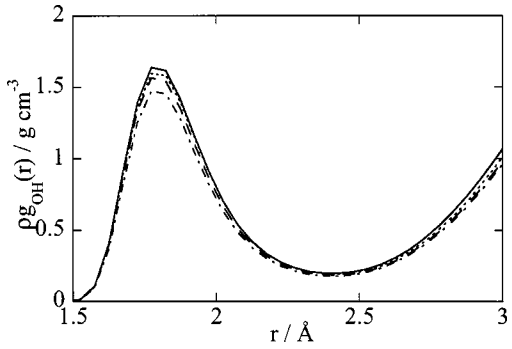

FIG. 9. Radial distribution functions between O and H atoms of the solvent water multiplied by the number density of the solvent, $\rho g_{\mathrm{OH}}(r)$. The solid, dotted, dashed, and dash-dotted curves are those of neat water and solutions of $\delta e=0$, $0.2541e$, and δe_0 ($=0.4238e$), respectively. It is to be noted that the function of $\delta e=\delta e_0$ (dash-dotted curve) is that of neat water (solid one) multiplied by 0.9.

C. Waterlike solute: Molecular dynamics simulation

The results of MD simulations on the solutions treated in the previous subsection are presented here in order to test the validity of our theoretical calculation.

Figure 9 compares $\rho g_{\mathrm{OH}}(r)$ of neat water and those of solutions. Comparing the hydrogen bonding peaks of solutions at $r=1.8$ Å, the peak height decreases with increasing the hydrophilicity of the solute (the value of δe), in harmony with our theoretical result shown in Fig. 7. However, those of solutions do not reach to the value of neat water.

Since the LJ core of the hydrogen atom is immersed in that of oxygen, the solute of $\delta e=0$ almost corresponds to that of the LJ solute in terms of the equilibrium structure. In consistency with Fig. 2(b), the hydrogen-bonding peak of solution of $\delta e=0$ is smaller than that of neat water. It means that the number of hydrogen bonding per a water molecule in the hydrophobic solution is smaller than that of neat water, if we define the ''number of hydrogen bonding'' by the coordination number.

The relative values of the self-diffusion coefficients and the single-particle reorientational times are plotted in Fig. 10 as a function of δe. The mobility of water increases first as the value of δe is decreased from the neat water value $0.4238e$. However, it has a turnover around $\delta e=0.3e$, and the solvent water becomes less mobile than the neat one at $\delta e<0.15e$. These trends in the simulation agree well with our theoretical prediction shown in Fig. 8. The mobility changes little at $\delta e<0.1e$, and it appears to increase slightly with decreasing δe, which is not reproduced in our theoretical calculation. We will, however, not pursue this discrepancy at present since the change in the mobility there is comparable to the simulation error.

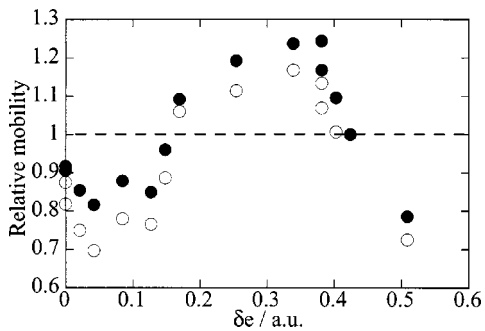

FIG. 10. Relative mobility of solvent water as a function of the partial charge of the solute, δe. The solid and open circles denote D/D_0 and $\tau_{\mu,0}/\tau_{\mu}$.

Anyway, the results of the MD simulation are consistent with our theoretical prediction as a whole in that the mobility of the solvent water has a maximum around $\delta e=0.3e$ as the function of δe, and it becomes smaller than that of neat water when the solute becomes strongly hydrophobic.

VI. CONCLUDING REMARKS

The transport properties and relaxation times of water in aqueous solutions are studied by the modified mode-coupling theory based on the interaction-site description. The slowing down of the solvent water is observed in the case of hydrophobic solutes, in harmony with many experimental and computer-simulation observations. The mechanism of the slowing down is analyzed and compared with that of the pressure dependence of the dynamic properties of neat water.[60] Both mechanisms are similar in that the increase in the number-density fluctuation in the low-q region enhances the electrostatic friction on the collective reorientation of the dipole moment. The increase in the number-density fluctuation is caused by the cavity formation by the solutes in the case of hydrophobic solution. The difference in the hydrophobic solution and the stretched water is that the solute can cause the repulsive friction on solvent water, which leads to the more pronounced slowing down.

Since the dynamic effects of the hydrophobic interaction result from the fluctuation, it depends quadratically on the difference between the strength of the solute–solvent and solvent–solvent interactions. On the other hand, there is an effect of the intermolecular interaction on average, which depends on the difference linearly. As a result of the competition of both effects, the mobility of water is enhanced by the slightly hydrophobic solutes, whereas it is reduced by the strongly hydrophobic one. The MD simulation on the same model is also performed, and the presence of the maximum in the dependence of the mobility of solvent water on the hydrophobicity of the solute is confirmed.

Some may consider that our approach to the dynamics of the hydrophobic hydration lacks a view that unifies the dynamics and thermodynamics of aqueous hydrophobic solutions. However, we believe that whether the unified picture is present is clarified after understanding both dynamics and thermodynamics. There is no doubt that both the dynamics and thermodynamics of the hydrophobic hydration are related to the structure of hydration. Since only the static structure is used as the input in our mode-coupling treatment, the change in structure is the reason for the slowing down of water also in our calculation. The relationship between microscopic structures and macroscopic properties of liquids is, however, so complicated that there is no guarantee at present that the dynamics and thermodynamics reflect the same part of the structure.

The slowing down of the solvent by nonpolar solute molecules is in fact not restricted to aqueous systems. Rather, similar behaviors are also found in the mixtures of nonpolar fluids and alcohols of low molecular weight,[21,86–89] although the formation of crystalline hydrates has not been reported in these systems so far as we know. We hope that our present theory may also help understanding the dynamics of solvophobic solvation in hydrogen-bonding systems in general.

ACKNOWLEDGMENT

This work was supported in part by the 21st Century COE Program ''Nature-Guided Materials Processing'' of the Ministry of Education, Culture, Sports, Science, and Technology.

[1] F. Franks, *Water: A comprehensive treatise*, edited by F. Franks (Plenum, New York, 1972), Vol. 4, Chap. 1, and references therein.
[2] W. Blokziji and J. B. F. N. Engberts, Angew. Chem., Int. Ed. Engl. **32**, 1545 (1993).
[3] J. A. V. Butler, Trans. Faraday Soc. **33**, 229 (1937).
[4] H. S. Frank and M. W. Evans, J. Chem. Phys. **13**, 507 (1945).
[5] R. A. Pierotti, Chem. Rev. **76**, 717 (1976).
[6] L. R. Pratt, Annu. Rev. Phys. Chem. **36**, 433 (1985).
[7] J. P. M. Postma, H. J. C. Berendsen, and J. R. Haak, Faraday Symp. Chem. Soc. **17**, 55 (1982).
[8] T. P. Straatsma, H. J. C. Berendsen, and J. P. M. Postma, J. Chem. Phys. **85**, 6720 (1986).
[9] D. A. Pearlman and P. A. Kollman, J. Chem. Phys. **90**, 2460 (1989).
[10] B. Guillot, Y. Guissani, and S. Bratos, J. Chem. Phys. **95**, 3643 (1991).
[11] B. Guillot and Y. Guissani, J. Chem. Phys. **99**, 8075 (1993).
[12] G. Kaminski, E. M. Duffy, T. Matsui, and W. L. Jorgensen, J. Phys. Chem. **98**, 13 077 (1994).
[13] E. C. Meng and P. A. Kollman, J. Phys. Chem. **100**, 11 460 (1996).
[14] J. W. Arthur and A. D. J. Haymet, J. Chem. Phys. **109**, 7991 (1999).
[15] K. A. T. Silverstein, A. D. J. Haymet, and K. A. Dill, J. Chem. Phys. **111**, 8000 (1999).
[16] J. Perkyns and B. M. Pettit, J. Phys. Chem. **100**, 1323 (1996).
[17] M. Kinoshita and F. Hirata, J. Chem. Phys. **106**, 5202 (1997).
[18] A. Kovalenko and F. Hirata, J. Chem. Phys. **113**, 2793 (2000).
[19] M. D. Zeidler, in *Water: A comprehensive treatise*, edited by F. Franks (Plenum, New York, 1972), Vol. 2, Chap. 12, and references therein.
[20] H. G. Hertz, Ber. Bunsenges. Phys. Chem. **68**, 907 (1964), and references therein.
[21] H. G. Hertz and M. D. Zeidler, Ber. Bunsenges. Phys. Chem. **68**, 821 (1964).
[22] E. von Goldammer and M. D. Zeidler, Ber. Bunsenges. Phys. Chem. **73**, 4 (1969).
[23] E. von Goldammer and H. G. Hertz, J. Phys. Chem. **74**, 3734 (1970).
[24] F. Franks, J. Ravenhill, P. A. Egelstaff, and D. I. Page, Proc. R. Soc. London, Ser. A **319**, 189 (1970).
[25] R. Haselmeier, M. Holz, W. Marbach, and H. Weingärtner, J. Phys. Chem. **99**, 2243 (1995).
[26] M. Nakahara and Y. Yoshimoto, J. Phys. Chem. **99**, 10 698 (1995).
[27] R. Ludwig, Chem. Phys. **195**, 329 (1995).
[28] U. Kaatze and R. Pottel, J. Mol. Liq. **52**, 181 (1992).
[29] G. H. Haggis, J. B. Hasted, and T. J. Buchanan, J. Chem. Phys. **20**, 1452 (1952).
[30] R. Pottel and U. Kaatze, Ber. Bunsenges. Phys. Chem. **73**, 437 (1969).
[31] K. Hallenga, J. R. Grigera, and H. J. C. Berendsen, J. Phys. Chem. **84**, 2381 (1980).
[32] T. Sato and R. Buchner, J. Chem. Phys. **119**, 10 789 (2003).
[33] A. Geiger, A. Rahman, and F. H. Stillinger, J. Chem. Phys. **70**, 263 (1979).
[34] P. J. Rossky and M. Karplus, J. Am. Chem. Soc. **101**, 1913 (1979).
[35] D. C. Rapaport and H. A. Scheraga, J. Phys. Chem. **86**, 873 (1982).
[36] D. A. Zichi and P. J. Rossky, J. Chem. Phys. **84**, 2814 (1986).
[37] J. Schnitker and A. Geiger, Z. Phys. Chem., Neue Folge **155**, 29 (1987).
[38] P. Linse, J. Am. Chem. Soc. **112**, 1744 (1990).
[39] A. Laaksonen and P. Stilbs, Mol. Phys. **74**, 747 (1991).
[40] A. K. Soper and J. L. Finney, Phys. Rev. Lett. **71**, 4346 (1993).
[41] J. L. Finney, A. K. Soper, and J. Z. Turner, Pure Appl. Chem. **65**, 2521 (1993).
[42] J. Turner and A. K. Soper, J. Chem. Phys. **101**, 6116 (1994).
[43] S. Dixit, J. Crain, W. C. K. Poon, J. L. Finney, and A. K. Soper, Nature (London) **416**, 829 (2002).
[44] A. Tani, Mol. Phys. **48**, 1229 (1983).
[45] L. Lue and D. Blankschtein, J. Phys. Chem. **96**, 8582 (1992).
[46] J. C. Owicki and H. A. Scheraga, J. Am. Chem. Soc. **99**, 7413 (1977).
[47] S. Swaminathan, S. W. Harrison, and D. L. Beveridge, J. Am. Chem. Soc. **100**, 5705 (1978).
[48] C. Pangali, M. Rao, and B. J. Berne, J. Chem. Phys. **71**, 2982 (1979).
[49] W. L. Jorgensen, J. Chem. Phys. **77**, 5757 (1982).
[50] I. I. Vaisman, F. K. Brown, and A. Tropsha, J. Phys. Chem. **98**, 5559 (1994).
[51] N. Matubayasi, J. Am. Chem. Soc. **116**, 1450 (1994).
[52] N. Matubayasi, L. H. Reed, and R. M. Levy, J. Phys. Chem. **98**, 10 640 (1994).
[53] R. L. Mancera, J. Chem. Soc., Faraday Trans. **92**, 2547 (1996).
[54] P.-L. Chau and R. L. Mancera, Mol. Phys. **96**, 109 (1999).
[55] S. Urahata and S. Canuto, Chem. Phys. Lett. **313**, 235 (1999).
[56] H. G. Hertz, *Water: A comprehensive treatise*, edited by F. Franks (Plenum, New York, 1972), Vol. 3, Chap. 7, and references therein.
[57] H. S. Frank and W.-Y. Wen, Discuss. Faraday Soc. **24**, 133 (1957).
[58] H. D. B. Jenkins and Y. Marcus, Chem. Rev. **95**, 2695 (1995), and references therein.
[59] O. Y. Samoilov, Discuss. Faraday Soc. **24**, 141 (1957).
[60] T. Yamaguchi, S.-H. Chong, and F. Hirata, J. Chem. Phys. **119**, 1021 (2003).
[61] T. Yamaguchi, A. Nagao, T. Matsuoka, and S. Koda, Chem. Phys. Lett. **374**, 556 (2003).
[62] T. Yamaguchi, A. Nagao, T. Matsuoka, and S. Koda, J. Chem. Phys. **119**, 11 306 (2003).
[63] D. Chandler and H. C. Andersen, J. Chem. Phys. **57**, 1930 (1972).
[64] F. Hirata and P. J. Rossky, Chem. Phys. Lett. **83**, 329 (1981).
[65] F. Hirata, M. B. Pettitt, and P. J. Rossky, J. Chem. Phys. **77**, 509 (1982).
[66] A. Kovalenko and F. Hirata, J. Chem. Phys. **110**, 10 095 (1999).
[67] S.-H. Chong and F. Hirata, Phys. Rev. E **58**, 7296 (1998).
[68] U. Balucani and M. Zoppi, *Dynamics of the Liquid State* (Clarendon, Oxford, 1994).
[69] J. Bosse and M. Henel, Ber. Bunsenges. Phys. Chem. **95**, 1007 (1991).
[70] J. Bosse and Y. Kaneko, Phys. Rev. Lett. **74**, 4023 (1995).
[71] S.-H. Chong and F. Hirata, Phys. Rev. E **58**, 6188 (1998).
[72] S.-H. Chong and W. Götze, Phys. Rev. E **65**, 041503 (2002).
[73] T. Yamaguchi and F. Hirata, J. Chem. Phys. **117**, 2216 (2002).
[74] T. Yamaguchi and F. Hirata, J. Chem. Phys. **115**, 9340 (2001).
[75] F. O. Raineri, Y. Zhou, H. L. Friedman, and G. Stell, Chem. Phys. **152**, 201 (1991).
[76] P. Madden and D. Kivelson, Adv. Chem. Phys. **56**, 467 (1984).
[77] S.-H. Chong, W. Götze, and M. R. Mayr, Phys. Rev. E **64**, 011503 (2001).
[78] T. Yamaguchi, S.-H. Chong, and F. Hirata, J. Mol. Liq. (to be published).
[79] H. J. J. C. Berendsen, J. R. Grigera, and T. P. Straatsma, J. Phys. Chem. **91**, 6269 (1987).
[80] P. J. Rossky, B. M. Pettitt, and G. Stell, Mol. Phys. **50**, 1263 (1983).
[81] J. Perkyns and B. M. Pettitt, J. Chem. Phys. **97**, 7656 (1992).
[82] A. Kovalenko, S. Ten-no, and F. Hirata, J. Phys. Chem. **20**, 928 (1999).
[83] M. P. Allen and D. J. Tildesley, *Computer Simulation of Liquids* (Oxford University Press, New York, 1987).
[84] N. Matubayasi and M. Nakahara, J. Chem. Phys. **110**, 3291 (1999).
[85] N. Matsubayashi and M. Nakahara, J. Chem. Phys. **94**, 653 (1991).
[86] M. A. Wendt and T. C. Farrar, Mol. Phys. **95**, 1077 (1998).
[87] R. Buchner and J. Barthel, J. Mol. Liq. **52**, 131 (1992).
[88] S. Schwerdtfeger, F. Köhler, R. Pottel, and U. Kaatze, J. Chem. Phys. **115**, 4186 (2001).
[89] R. L. Smith, Jr., C. Saito, S. Suzuki, S.-B. Lee, H. Inomata, and K. Arai, Fluid Phase Equilib. **194–197**, 869 (2002).